Seasonal Hydrodynamics and Salt Exchange of a Shallow Estuary in Northern China

Authors: Zou, Tao, Zhang, Hua, Meng, Qingjia, and Li, Jia

Source: Journal of Coastal Research, 74(sp1) : 95-103

Published By: Coastal Education and Research Foundation

URL: https://doi.org/10.2112/SI74-009.1

Journal of Coastal Research	SI	74	95–103	Coconut Creek, Florida	2016

Seasonal Hydrodynamics and Salt Exchange of a Shallow Estuary in Northern China

Tao Zou[†‡], Hua Zhang[‡*], Qingjia Meng[#] and Jia Li[‡]

[†] Key Laboratory of Marine Ecology and Environmental Sciences
Institute of Oceanology
Chinese Academy of Sciences
Qingdao, Shandong 266071, P. R. China

[‡] Key Laboratory of Coastal Environmental Processes and Ecological Remediation
Yantai Institute of Coastal Zone Research
Chinese Academy of Sciences
Yantai, Shandong 264003, P. R. China

[#] Chinese Research Academy of Environmental Sciences
Beijing, 100012, P. R. China

www. cerf-jcr. org

www. JCRonline. org

ABSTRACT

Zou, T.; Zhang, H.; Meng, Q. J., and Li, J., 2016. Seasonal hydrodynamics and salt exchange of a shallow estuary in Northern China. *In*: Harff, J. and Zhang, H. (eds.), *Environmental Processes and the Natural and Anthropogenic Forcing in the Bohai Sea, Eastern Asia. Journal of Coastal Research*, Special Issue, No. 74, pp. 95–103. Coconut Creek (Florida), ISSN 0749–0208.

Estuaries are important components of coastal ecosystem and function as dominant pathways of material exchange at the land-sea interface. The transport of terrestrial input through river inflow is controlled by physical process including tides, waves, and fresh water discharge. This study investigates hydrodynamic characteristic and salt flux within Xiaoqinghe River (XQR) estuary, which is a shallow estuarine system (water depth < 8 m) and exports substantial amount of nutrients and pollutants to the adjacent Laizhou Bay. Profile velocity and salinity are measured using ADCP and CTD through complete tidal cycles (25 hours) in April, July and September 2013. The instantaneous velocity and salinity data are decomposed into time-averaged means and time-varying components based on the improved Kjerfve (1986) method to quantify the contributions of various physical processes. The results showed that the XQR estuary had irregular semidiurnal tide with tidal form number of 0.5–0.7 and tidal range about 2 m. River discharge dominated the seasonal variation of tidal elevation, longitudinal velocity, and salinity. The river mouth was well mixed based on calculated layer Richardson number, and can be classified as Type 1b and 2b according to stratification-circulation diagram. The net salt flux was directed seaward during monsoon season and landward in non-monsoon seasons. Fluvial advective flow dominated the seaward salt flux throughout the year and contributed 78.9% of the net salt flux in monsoon. Stokes' drift and tidal sloshing dispersion flux dominated the landward salt flux, and contributed 72% and 57.5% of total salt flux in April and September, respectively. The cross-correlation between tide and salinity, and vertical shear, were only of marginal importance. Overall, tidal sloshing and Stokes' drift is the underlying process of salt transport while river discharge dominates its seasonal variation. This study revealed the inherent unsteadiness of the salt balance, and provided the scientific foundation for effective management of freshwater release from upstream during difference seasons.

ADDITIONAL INDEX WORDS: *Stratification, slat flux, estuary, Xiaoqinghe River, classification.*

INTRODUCTION

Estuaries at the land-sea interface are critical zones in the functioning of coastal ecosystem. Many estuaries are highly productive environments and important routes through which terrestrial material enter the ocean (Simpson *et al.*, 2001). Estuaries are highly dynamic environments with their physical, chemical and biological structure characterized by high spatial and temporal variability (Valle-Levinson, 2010). Increasing population and economic activities around estuaries have caused severe stress to their environmental and ecological functions. Excessive nutrients and pollutants discharging into coastal waters damaged or destroyed natural habitats (Halpern *et al.*, 2008) and caused coastal ecosystem degradation such as hypoxia and eutrophication (Wolanski, 2007). To understand the interaction between land and ocean, increasing research efforts have been diverted to study fluxes of bio-geochemically active components through estuarine system (Simpson *et al.*, 2001), which are dependent on the transport processes (Kasai *et al.*, 2010).

Hydrodynamic properties and net salt fluxes are critical parameters for modeling biogeochemical and water quality processes in estuaries. To understand water and salt exchange, it is important to study hydrodynamic factors controlling the total longitudinal flux (Officer and Kester, 1991). Estuarine hydrodynamics is

DOI: 10.2112/SI74-009.1 received (26 January 2015); accepted in revision (2 July 2015).

*Corresponding author; hzhang@yic.ac.cn

controlled by riverine factors (river discharge), marine factors (tides, waves, and currents), meteorological factors (winds, atmospheric pressure, and temperature variability), and geomorphologic factors (topography and bathymetry) (Sierra *et al.*, 2002). Understanding salt exchange mechanism is the basis for predicting the transport of nutrients, pollutants, and planktonic organisms. Previous studies showed that net salt flux is a balance of advection flux and a number of dispersive fluxes, including tide effect, shear effect and turbulence effect. The tidal effects are component of tidal sloshing, Stokes drift and cross-correlation between tide and salinity (Kjerfve, 1986; Miranda *et al.*, 2012; Restrepo and Kjerfve, 2002). In steady-state, there is a balance between seaward advection of fluvial discharge and landward dispersion of saltier ocean water (Hunkins, 1981; Miranda and Kjerfve, 1998; Siegle *et al.*, 2009; Simpson *et al.*, 1997; Uncles and Lewis, 2001). The landward salt transport is a consequence of dispersion produced by tidal and wind mixing and by horizontal density gradient (Vaz, Lencart and Dias, 2012). Tidal sloshing is the triple correlation between tidal depth changes, tidal currents and tidal salinity changes. It is the dominant dispersive flux in well mixing estuary (Cavalcante *et al.*, 2013; Kjerfve, 1986; Siegle *et al.*, 2009). Stokes drift dispersion can be at same order of magnitude as advective salt transport due to freshwater discharge in Severn and Camboriu estuaries (Siegle *et al.*, 2009; Uncles and Jordan, 1979). It is the dominant dispersive salt flux during high discharge conditions in Hudson River estuary (Geyer and Nepf, 1996), an order of magnitude lower than river discharge in Vassova lagoon (Sylaios *et al.*, 2006), insignificant in lower reaches of the Tamar estuary (Uncles *et al.*, 1985). In most studies, the vertical shear effect contribution was considered negligible (Ali *et al.*, 2010; Uncles and Lewis, 2001). But in some lower reaches at neap tides it can be an important flux (Uncles *et al.*, 1985).

The mechanism of salt transport does not only vary between different estuaries, but also depend on spring and neap tidal cycles, and river discharge conditions. For example, observations along the Tamar Estuary demonstrated that tidal pumping and vertical shear dominated at spring and neap tides, respectively (Uncles *et al.*, 1985). The vertical shear flux at neap tides exceeded that at spring tides in lower reaches of Tamar estuary (Uncles and Lewis, 2001). The direction of Stokes' drift flux may be different in spring and neap tides, with upstream in neap tide and downstream in spring tide (Siegle *et al.*, 2009). The difference between lower and upper reaches is mainly due to tidal range variability and local morphology (Cavalcante *et al.*, 2013; Park and James, 1990). Tidal pumping is insignificant during low discharge conditions compared to high discharge conditions in Hudson River estuary (Geyer and Nepf, 1996). In general, net salt flux varied both spatially and temporarily with changing hydro-morphological and meteorological conditions (Ali *et al.*, 2010). Understanding the control mechanism of salt transport in different zone of estuarine system helps to explain how natural and anthropogenic changes to the ecosystem affect it capacity to flush pollutants (Vaz *et al.*, 2012).

The objective of this study is to investigate the hydrodynamic properties and salt transport characteristics of Xiaoqinghe River (XQR) estuary based on profile measurement of salinity, velocity, and elevation over tidal cycles at different run-off conditions. Tidal harmonic constants, stratification and net salt flux were calculated to determine the dominant components of salt transport. This study would provide better understanding of physical process of the estuary, which is essential for future planning on ecological and environmental restoration and remediation in this region.

MATERIAL AND METHODS

Study site

The XQR is located in the southwestern corner of Laizhou Bay (LZB), which is the southern portion of Bohai Sea (Figure 1). The length of the XQR is 240 km with the basin area of 11 000 km^2. The river has 900 years of history since the artiflcial excavation made in the Southern Song Dynasty. The lower river reach of XQR starts from WangDao, the last sluice, is a strong-tidal channel with anomalous semidiurnal tides. This section of XQR estuary is about 200 km^2, with depth from 3.5 to ~6 m.

The XQR watershed is highly industrialized and strongly influenced by human activity. Water quality and ecosystem health in the river are degraded by pollutants from industrial, agricultural, municipal and stormwater sources (Ma *et al.*, 2004; Zhuang and Gao, 2014). XQR is the main pollution sources causing the ecological deterioration in LZB (Cui *et al.*, 2003; Jin *et al.*, 2012; Luo *et al.*, 2013). Excessive organochlorine pesticides, Polychlorinated naphthalenes (PCNs), Polybrominated diphenyl ethers (PBDEs), antibiotics and nutrient runoff from XQR watershed has caused serious harmful impact on the estuary (Ji *et al.*, 2007; Pan *et al.*, 2011; Xia and Zhang, 2011; Zhang *et al.*, 2012; Zhong *et al.*, 2011).

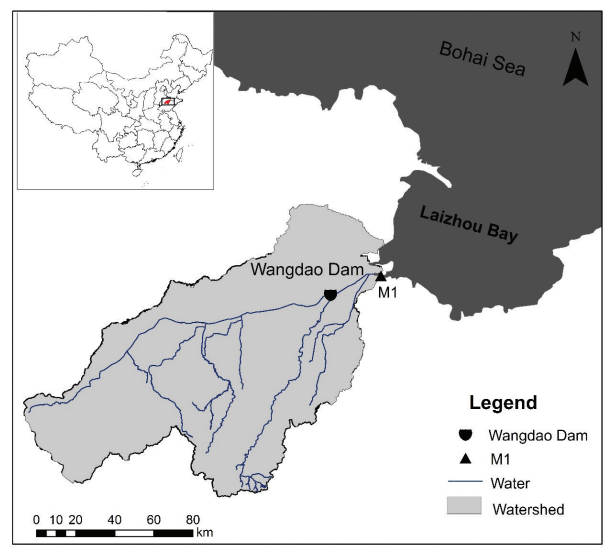

Figure 1. Location Map of the study site, Xiaoqinghe River Estuary (southwest of the Bohai Sea, north of China)

Current and Salinity Measurements

Field measurements at M1 station (37.295° N, 119.008° E) were carried out for 25 hours continual monitoring of XQR estuary (Figure 1). To reveal the temporal variation of hydrodynamic properties and net salt flux in XQR estuary, the measurement was conducted in April, July and September 2013 (Table 1), which

is before, during and after East Asian Summer Monsoon, respectively. The stationed instrument packages consisted of a Conductivity, Temperature and Depth probe (CTD) and Acoustic Doppler Current Profile (ADCP). Temperature, salinity and press were measured with a RBR XR-620 CTD (in April and July) and SST CTD60 (in September) with a sample frequency of 1Hz. The CTD was deployed to get vertical physical structure of the water column once an hour. In additional, we also deployed another RBR XR-420 CTD at the surface and the bottom in April and July. A Teledyne RDI's ADCP Workhorse Sentinel with 614.4 KHz was used to measure current profile, including velocity magnitude and direction. The ADCP was set up at the side of a wooden fishing ship using a stainless steel frame and its transducers were maintained at 0.2 m depth below the sea surface. The ADCP was programmed to 20 bins with 0.25 m bin size and 120s ensemble interval, blanking range of 0.9 m. River flow data were obtained from China Hydrology (available at http://xxfb.hydroinfo.gov.cn/index.html). There was no precipitation during three surveys, and evaporation and wind was neglected. The time, tidal, river flow and salinity characteristics for the three surveys are summarized in Table 1.

Table 1. *Summary of time, tidal and river discharge conditions in three surveys*

Date		Tide	River flow*	Water	Salinity range
Start	End		(m^3/s)	level(m)	(PSU)
26-Apr-2013 17:30	27-Apr-2013 18:00	Spring	18	3.5~5.8	9.60~21.75
13-Jul-2013 16:00	14-Jul-2013 16:30	Neap	180	4.4~6.2	1.80~4.27
27-Sep-2013 09:00	28-Sep-2013 09:30	Neap	40	4.0~5.9	4.25~14.98

Note: the river flow is referenced to the Shicun hydrologic station, located at downstream of XQR.

Stratification and stability

Stratification is a ubiquitous phenomenon in the mixing zone of an estuary suffering from saltwater intrusion. It can enhance gravity current, strengthen saltwater sailing upstream to some degree and play a fundamental role in the salt balance (Nepf and Geyer, 1996). Intensity of stratification is characterized by stratification index $N=\delta S/S_0$, where S_0 is the vertically averaged salinity, and δS is the top-to-bottom salinity difference (Hansen and Rattray, 1966; Haralambidou *et al.*, 2010). In case $N < 0.1$, the water column is fully mixed, when $0.1 < N < 1.0$ then partial mixing occurs, while $N > 1.0$ indicates stratification.

Similarly to stratification parameter N, the Froude number is the ratio of the flow speed to the speed of long gravity waves (Armi and Farmer, 1986). The internal densimetric Froude number Fr is calculated as,

$$F_r = \frac{V}{\sqrt{g'h}}, \text{ and } g' = g\frac{\Delta\rho}{\rho} \quad (1)$$

where V is longitudinal velocity. g' is reduced gravity, $\Delta\rho$ is density difference between surface and bottom, and ρ is depth-averaged density of water column (Stommel and Farmer, 1952).

Water column stability is examined using the gradient Richardson number Ri_g (Richardson, 1920) or bulk Richardson number Ri_L (Dyer, 1982; Ellison and Turner, 1959):

$$Ri_g = \frac{g(\frac{\partial\rho}{\partial z})}{\rho(\frac{\partial V}{\partial z})^2}, \text{ or } Ri_L = \frac{g'h}{\bar{V}^2} \quad (2)$$

where $\partial\rho/\partial z$ is the vertical density gradient, $\partial V/\partial z$ is the vertical gradient of longitudinal velocity, and $\bar{V}$ is the depth-averaged longitudinal velocity. In conditions such as ours, where the density gradients is not got precisely, the bulk Richardson number Ri_L can be used (Vaz *et al.*, 2012). $Ri_L = 20$ is defined as the upper limit for the occurrence of turbulent mixing in partially mixed estuaries (Dyer, 1982).

Salt fluxes

Total salt flux within an estuarine system is typically determined using velocity and salinity measured at locations along a vertical section. In general, the longitudinal net salt fluxes (F) per unit width perpendicular to the mean flow may be calculated as (Bowden, 1963; Kjerfve, 1986; Dyer, 1997; Restrepo and Kjerfve, 2002)

$$F = \int_0^h [V(z)S(z)]\,dz \quad (3)$$

where h is water depth (cm), $V(z)$ represents the observed longitudinal velocity (cm/s), $S(z)$ represents the observed salinity (PSU) and z is the vertical coordinate.

In the case of tidal flow, following the procedure similar to the previous studies (Ali *et al.*, 2010; Bowden, 1963; Hunkins, 1981; Uncles and Lewis, 2001), the instantaneous velocity and salinity can be decomposed into term that represent the physical process responsible for the advective and dispersive mass transport. For a lateral homogeneous estuarine channel velocity (V) and salinity (S) are decomposed as:

$$\begin{cases} V = \bar{V} + V' \\ S = \bar{S} + S' \end{cases} \quad (4)$$

where $\bar{V}$ and $\bar{S}$ are depth-averaged velocity and salinity, and V' and S' are deviations from $\bar{V}$ and $\bar{S}$. The depth-averaged means are decomposed into time-averaged and a time varying components. Eq. (4) can be written as

$$\begin{cases} V = \bar{V} + V' = \langle\bar{V}\rangle + V_T(t) + V' \\ S = \bar{S} + S' = \langle\bar{S}\rangle + S_T(t) + S' \end{cases} \quad (5)$$

where angle brackets are net, or time-averaged over at least one complete tidal cycle.

The local water depth h varies with the tidal elevation and can be decomposed into the time-averaged water depth and the tidal height (Vaz *et al.*, 2012):

$$h(t) = \langle h\rangle + h_T(t) \quad (6)$$

Substituting Eq. (5) and Eq. (6) into Eq. (3), the net longitudinal salt flux for one or more complete tidal cycles can be expressed as

$$\langle F\rangle = \langle h\rangle\langle\bar{V}\rangle\langle\bar{S}\rangle + \langle hV_tS_t\rangle + \langle\bar{V}\rangle\langle h_tS_t\rangle + \langle\bar{S}\rangle\langle h_tV_t\rangle + \langle hV'S'\rangle \quad (7)$$

for simplicity, it can be written as

$$Net\ Flux = Flux\ 1 + Flux\ 2 + Flux\ 3 + Flux\ 4 + Flux\ 5 \quad (8)$$

Each decomposed flux represents the related physical process (Bowden, 1963; Kjerfve, 1986; Restrepo and Kjerfve, 2002).

Flux 1 is the Eulerian residual transport flux, which account for the advective flux due to fluvial discharge. The other 4 fluxes are dispersive in nature. *Flux* 2 is the tidal sloshing effect caused by the triple correlation between tidal depth change, tidal current and tidal salinity change, and is usually the dominant dispersive flux. *Flux* 3 is the cross-correlation between tide and salinity. *Flux* 4 is the Stokes' drift dispersion. *Flux* 5 is the shear flux due to gravitational circulation. For well-mix estuary system, the gravitational circulation is usually negligible and *Flux* 5 is considered insignificant (Ali *et al.*, 2010; Kjerfve, 1986), while the *Flux* 5 is significant in the estuaries with vertical stratification (Bowden, 1963; Restrepo and Kjerfve, 2002).

RESULT AND DISCUSSION

Tidal, salinity and currents variation

The time series of tidal elevation, salinity and longitudinal velocity in three surveys were shown in Figure 2. Tidal elevations showed that there were two flood tides and ebb tides during each survey. The tidal elevation between the adjoining flood tides was significantly different, suggesting tidal asymmetry in XQR estuary. Using the tidal quasi-harmonic method for short term data (Parker, 2007), the harmonic coefficients of tidal constituents M_2, S_2, O_1, K_1, M_4, and MS_4 were calculated and given in Table 2. A difference-ratio at Reference Station (Weifang Port) was used. The results showed that M_2, S_2, K_1 and O_1 were the dominant constituents. Calculated tidal form numbers, the ratio of the main diurnal and semidiurnal component amplitudes, $(K_1+O_1)/(M_2+S_2)$ (Defant, 1960), were 0.5, 0.7 and 0.6, respectively, which showed that the tide were irregular semidiurnal. There were considerable seasonal variations in tidal ranges, which were 2.3 m, 1.8 m and 1.9 m in April, July and September, respectively. The smallest tidal range was in July due to the neap tide and high river discharge (180 m^3/s).

The time series of depth-averaged longitudinal velocity had similar pattern as that of water level in each survey (Figure 2) with 3h time lag, indicative of a standing wave tidal regime. The longitudinal velocity varied from −70.8 cm/s to 74.4 cm/s in April, from −41.9 cm/s to 96.5 cm/s in July and from −81.3 cm/s to 63.4 cm/s in September. The depth-averaged longitudinal velocity indicated a strong asymmetry in intra tidal and seasonal timescale. Due to high freshwater discharge in July, the maximum ebb current was bigger than the maximum flood current, with an Eulerian residual velocity up to 37.3 cm/s. In April and September surveys, the velocity asymmetry was mainly reflected in the difference between two flood/ebb currents.

Table 2. *Main water level tidal harmonic constants in XQR Estuary, where H(cm) is amplitude and g(°) is the phase*

Constituent		Period	April		July		September	
			H(cm)	g(°)	H(cm)	g(°)	H(cm)	g(°)
Semidiurnal	M_2	12.42	89.5	127.1	65.2	117.8	77.1	90.2
	S_2	12.00	20.8	179.6	18.9	186.8	22.3	159.2
Diurnal	O_1	25.82	22.5	18.5	17.6	25.2	21.4	10.2
	K_1	23.93	28.8	65.5	23.2	78.3	28.3	63.2
Shallow water	$M4$	6.21	12.3	80.2	6.0	106.2	20.9	74.5
	MS_4	6.10	8.6	135.5	3.5	175.2	12.1	143.5

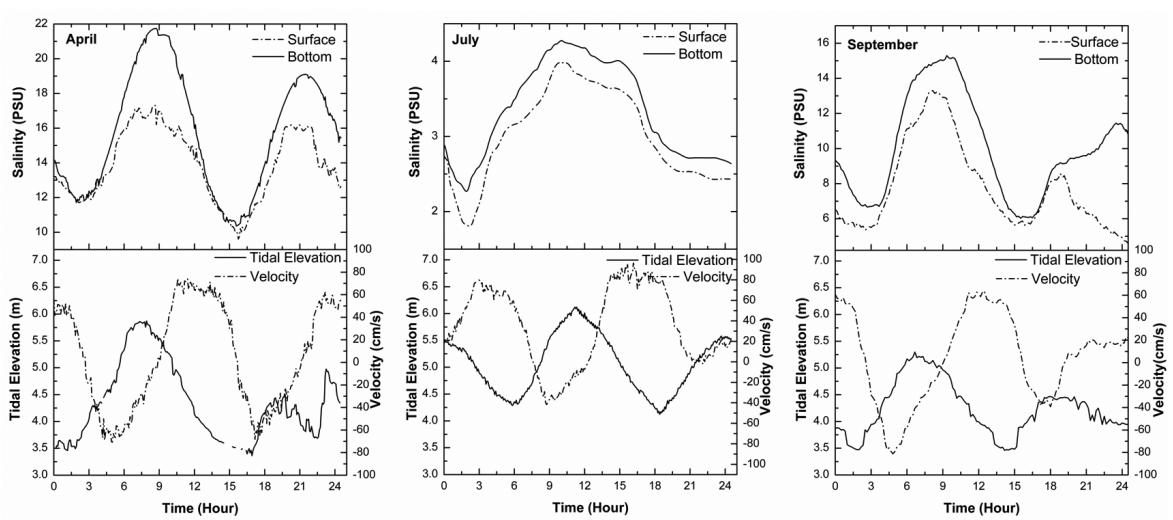

Figure 2. Tidal elevation, depth-averaged longitudinal velocity and salinity at surface and bottom variation in three surveys

The profiles of tide-averaged longitudinal velocity (Figure 3) showed similar trend. The velocities were positive at the surface (seaward flow) and negative at the bottom (landward flow). The residual velocities varied from 15.2 cm/s at surface to −32.1 cm/s at bottom in April and from 19.2 cm/s at surface to −28.7 cm/s at bottom in September. Under the high river discharge conditions (in July), the residual velocities were positive (seaward) from surface (52.0 cm/s) to bottom (5.1 cm/s), reflecting that the river discharge dominated the advective flow from surface to bottom. The circulation parameter calculated as net surface velocity (V_s) divided by depth-averaged velocity (V_f) (Hansen and Rattray, 1966) was 2.8, 1.3 and 3.3 in April, July and September, respectively, indicating that gravitational circulation was weak in July and slightly more pronounced in April and September. The profiles of tide-averaged longitudinal velocity also indicated that the shear existed in three surveys.

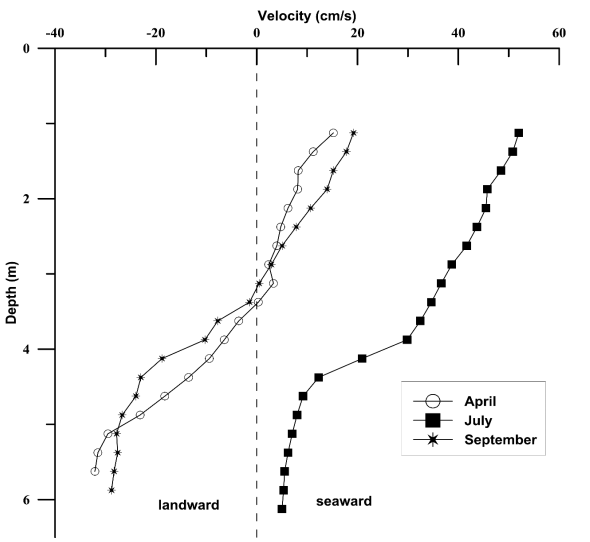

Figure 3. Profile of tide-averaged longitudinal velocity in three surveys

The salinity ranges (Table 1 and Figure 2) showed strong seasonal variation, with 12.5 PSU, 2.47 PSU and 10.73 PSU in April, July and September, respectively. The low salinity range in July resulted from heavy rainfall brought by East Asian Summer Monsoon. The salinity variations both at surface and bottom were consistent, with higher range colse to the bottom. The temporal variation of salinity followed the one of tidal elevation under low river discharge condition, with the maximum salinity occurring close to high water level and average values being greater in April. In addition, the difference (δS) between surface and bottom water was higher in spring tide than in neap tide, and higher in flood tide than in ebb tide. And the difference also offered a clear evidence of gravitational circulation.

Stratification and stability

The stratification index N was found to be below 0.4 in all three surveys except during last 4 hours in September (0.4–0.8). It suggested that XQR estuary was partial mixing system. During the high discharge condition in July, the XQR estuary was well mixing system with the stratification index N below 0.1, indicating that the high river runoff resulting in the weak stratification and well mixing in XQR estuary. The variation of N-values (Figure 4) was consistent with the tidal level in April and September, with minimum stratification value at the end of ebb tidal phase and maximum at the end of flood tidal phase. As instantaneous salinity stratification was dependent on interfacial shear, the relative lower flood shear stresses (compared to the corresponding ebb shear) explain the stratification variability during tidal phase (Haralambidou *et al.*, 2010). These were evidence of tidal straining occurring through each tidal cycle. In July, the velocity of freshwater flow was about 50cm/s, showing that the freshwater runoff dominated the current profile and resulted in lower shear stress with less than 0.1 N value. All above reflected the dominance of freshwater runoff in July and tide in spring and autumn. Wind contributed to some extent in the third survey to enhance the stratification. The Froude number Fr was always lower, ranging from 0.2 to 0.3. Calculated layer Richardson number Ri_L (Figure 5) was less than 2 except during flood tide, indicating that mixing was fully developed. The relatively strong stratification ($Ri_L > 20$) at flood tide can be explained by the reduction in current flow (slack tide) and increase in salinity gradient.

According to the classical stratification-circulation diagram classification (Hansen and Rattray, 1966) on the assumption of laterally homogeneous condition, the XQR estuary was classified as Type 2b, Type 1b and Type 2b in April, July and September, respectively (Figure 5). Type 1b characteristic of net seaward flow at all depths and appreciable stratification, and Type 2b characteristic of net flow reversing at depth and both advection and diffusion contributing import to the upstream salt flux, also were evidenced by Figure 3 and Figure 5. This indicated that the tidal diffusion was the main process for the landward salt transport in April and September, meanwhile, the advection was the main process for seaward in July.

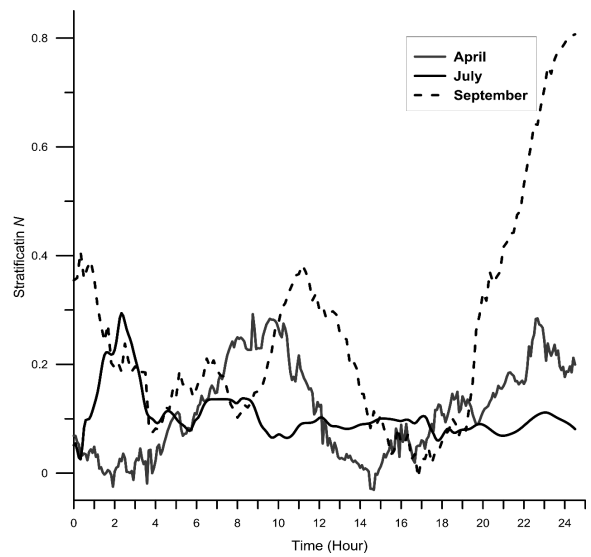

Figure 4. Calculated stratification index in three surveys

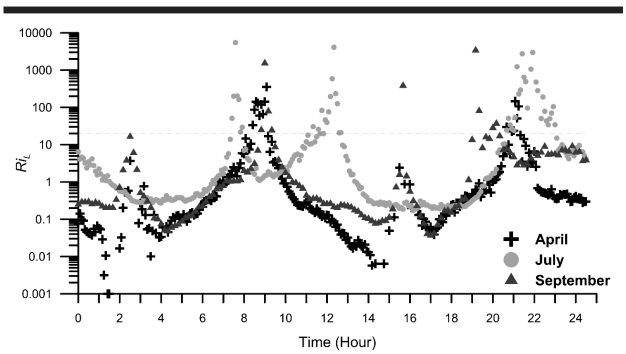

Figure 5. Intra tidal variation of the layer Richardson number (Ri_L)

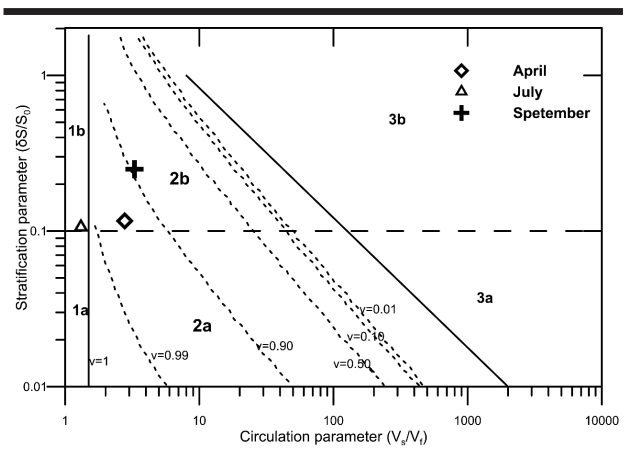

Figure 6. Classification of the estuary of XQR estuary in three surveys according to the diagram of Hansen and Rattray (1966)

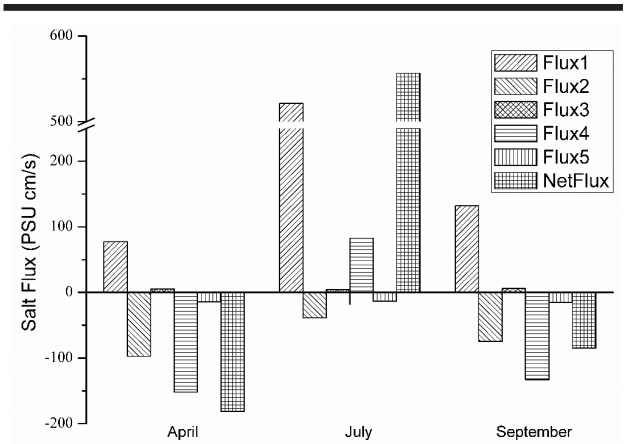

Figure 7. The salt flux at XQR Estuary in April, July and September

Salt fluxes and processes

Salt fluxes calculated based on Eq. 5 were summarized in Figure 7 for the three surveys. Overall, there was a net seaward flux in July and a net landward flux in April and September. In July, *Flux* 1 (net advective salt flux) dominated the salt flux with a value of 521.4 PSU cm/s, contributing 78.9% of total flux and 93.6% of seaward flux. The other four fluxes were relatively small with the highest being *Flux* 4 (Stokes' drift flux) of 82.6 PSU cm/s. In April and September, the net salt flux was directed landward with net fluxes of −181.1 and −84.9 PSU cm/s, respectively. Due to lower freshwater discharge, *Flux* 1 contributed only 22.3% and 33.6% of total flux in April and September respectively. In both surveys, *Flux* 4 was the predominant flux with values of 152.0 and 133.1 PSU cm/s. *Flux* 4, representing the Stokes' drift dispersion, was directed landward and provided the biggest landward salt flux. In addition, *Flux* 2, representing the tidal sloshing effect, also contributed a substantial fraction of landward flux with values of 97.3 and 74.5 PSU cm/s, respectively. Overall, stokes' drift and tidal dispersion were dominate components in total upstream salt transport, and contribute 72% and 57.5% to total salt flux in April and September. The rest two fluxes, *Flux* 3 and *Flux* 5, were relatively small in comparison with *Fluxes* 1, 2, and 4. *Flux* 3 (cross-correlation flux) contributed less than 2% and directed seaward for all three surveys. *Flux* 5 (shear flux) contributed less than 5% of net salt flux and directed landward.

The results showed that there were pronounced differences in total salt transport among three surveys. In monsoon, the total salt flux was directed downstream (seaward), contrary to upstream transport (landward) in pre and post monsoon. During monsoon, which account for about 80% of annual precipitation (Gao *et al.*, 2008; Tsur, 2004), the freshwater discharge could be up to about 180 m^3/s, with residual velocity of 37.3 cm/s. Due to high runoff, freshwater discharge dominated the flow of the whole water column with the tide-averaged current directing seaward. It was consistent with observed high water level and low salinity in Figure 2 and classification of 1b in stratification-circulation diagram, indicating that *Flux* 1 fully dominated net salt flux. This process was also by far the most significant advective component of the seaward salt flux in XQR estuary through the whole year, and contributed 22.3% and 33.6% of total salt flux in April and September, respectively. In pre and post monsoon with low runoff, freshwater discharge dominated the seaward salt flux, but was not the principal component of the net salt flux. Instead, Stokes' drift and tidal sloshing dispersion dominated net salt flux and caused the net salt flux seaward. The balance between fluvial discharge, Stokes' drift and tidal sloshing dispersion controlled landward and seaward salt transport, and determined the direction and magnitude of net salt flux, similar to previous studies in other estuaries (Cavalcante *et al.*, 2013; Restrepo and Kjerfve, 2002; Siegle *et al.*, 2009).

Stokes' drift dispersion was the biggest landward salt flux and dominated the net salt flux during non-monsoon. The Stokes' drift directed landward except in July. The importance of Stokes drift within XQR estuary system can be explained by the stronger and longer flood currents. Meanwhile, Stokes' drift was higher in spring tide than that in neap tide, which may be explained by stronger currents in spring tide but further evidence will be needed. Tidal sloshing was usually the major landward flux component in well-mixed systems (Kjerfve, 1986). Its value was often controlled by stratification. Thus the overall *Flux* 2 was largely a function of tidal sloshing, coinciding with the V_T, S_T

(Eq. 3) function of tidal cycle. Stratification and stability analysis in Figure 4, 5, 6 showed that the XQR estuary was partially to fully mixed estuary with stratification existed only in flood tide. In three surveys, the tidal dispersion flux was landward. Higher value in April coincided with higher stratification. Similarly to Stokes' drift, there was no direct relation with spring-neap tide variations, although stratification could partially explain the high dispersion flux in April.

Overall, *Flux* 1, which directed seaward and controlled by freshwater discharge, was the most significant component in monsoon, and controlled the seasonal variation of net salt flux. *Flux* 2 and *Flux* 4 were the major component in non-monsoon seasons, during which the landward salt transport as a result of tides was the dominant process within XQR estuary. In addition, *Flux* 1 was also an important component along with tidal dispersion and Stokes' drift to dominate net salt transport and salt intrusions in April and September. In comparison, *Flux* 3 and *Flux* 5 were insignificant in all three events.

In the absence of meteorological data, this study fail to give information about meteorological effect on salt transport, especially the contribution of wind. And the measurement campaigns were too short to give the direct relations between salt fluxes and spring-neap tidal variation. It should be noted that the seaward salt flux might be underestimated due to the absence of velocity data at surface layer where the tide-averaged current is directed seaward (Figure 3).

Although there is some uncertainties, all results reveal an imbalance in the net salt budget and the variation of salt exchange in XQR estuary in pre-monsoon, monsoon and post-monsoon season in 2013. This imbalance may be mainly due to a strong variation of river discharge. In general, salinity is considered to be natural tracer, and the salt transport and exchange could be linked to the transport mechanisms of contaminated water in the estuary system. The mechanism of salt transport and exchange could help to explain the capacity to flush pollutant. Furthermore, as we know, the lower river reach of XQR starts form WangDao, which is the last sluice (Figure 1). Because the *flux* 1 was the most significant component in monsoon, and controlled the seasonal variation of net salt flux, it is possibility to change net salt flux by regulating freshwater discharge flux at WangDao. Therefore, this study could provide the scientific foundation for effective management of freshwater release.

CONCLUSIONS

Current profile characteristic and salt balance of Xiaoqinghe River estuary were characterized using 25 hours CTD and ADCP observations in April, July and September of 2013. Results showed that the XQR estuary had irregular semidiurnal tide with tidal form number of 0.5–0.7 and tidal range about 2 m. The river discharge dominated the seasonal variation of tidal elevation, longitudinal velocity and salinity. The stratification index, Froude number and Richardson number also indicated that the river mouth was well mixed. The XQR estuary can be classified as Type 1b and 2b according to stratification-circulation diagram.

XQR estuary was characterized by seasonal variation in net salt transport. The net salt flux was a balance between advective freshwater discharge, Stokes' drift, and tidal sloshing dispersion, and was directed seaward during monsoon season and landward in non-monsoon seasons. The predominant seaward transport of salt was dominated by river discharge throughout the year, with Stokes' drift also presenting a net seaward flux in monsoon. Fluvial advective flow contributed 78.9% of total salt flux in monsoon and contributed 22.3% in April and 33.6% in September. Stokes' drift and tidal sloshing dispersion flux dominated the landward salt flux, and contributed 72% and 57.5% of total salt flux in April and September, respectively. The other two components, i. e., *Flux* 3 and *Flux* 5, were only of marginal importance. Tidal sloshing and Stokes' drift was the underlying process of salt transport while river discharge dominated its seasonal variation, and direction reverse of Stokes' drift (seaward during monsoon and landward during non-monsoon seasons). This study provided the scientific foundation for effective management of freshwater release from upstream during difference seasons, and revealed the inherent unsteadiness of the salt balance over the XQR estuary, which warrants further experimental and modelling studies to quantify the transport processes in a variety of seasonal and spring-neap cycles.

ACKNOWLEDGMENTS

The authors thank Qiong Wang for creating Figure 1. This research was supported by the Key Deployment Project of the Chinese Academy of Sciences (KZZD-EW-14), National Natural Science Foundation of China (No. 41406029), NSFC-Shandong Joint Fund (U1406403), and the Strategic Priority Research Program of the Chinese Academy of Sciences (XDA11020305).

LITERATURE CITED

Ali, A.; Lemckert, C. J., and Dunn, R. J. K., 2010. Salt fluxes within a very shallow subtropical estuary. *Journal of Coastal Research*, 26(3), 436–443.

Armi, L. and Farmer, D. M., 1986. Maximal two-layer exchange through a contraction with barotropic net flow. *Journal of Fluid Mechanics*, 164(1), 27–51.

Bowden, K. F., 1963. The mixing processes in a tidal estuary. *International Journal of Air Water Pollution*, 7, 343–356.

Cavalcante, G. H.; Feary, D. A., and Kjerfve, B., 2013. Effects of tidal range variability and local morphology on hydrodynamic behavior and salinity structure in the Caeté river estuary, north Brazil. *International Journal of Oceanography*, 2013, 1–10.

Cui, Y.; Ma, S.; Li, Y.; Xing, H.; Wang, M.; Xin, F.; Chen, J., and Sun, Y., 2003. Pollution situation in the Laizhou bay and its effects on fishery resources. *Marine Fisheries Research (China)*, 24(01), 35–41 (Chinese with English abstract).

Defant, A., 1960. *Physical Oceanography*. Oxford: Pergamon Press, 598p.

Dyer, K. R., 1997. *Estuaries: a physical introduction*. New York: Wiley, 175p.

Dyer, K. R., 1982. Mixing caused by lateral internal seiching within a partially mixed estuary. *Estuarine, Coastal and Shelf Science*, 15(4), 443–457.

Ellison, T. H. and Turner, J. S., 1959. Turbulent entrainment in stratified flows. *Journal of Fluid Mechanics*, 6(3), 423–448.

Gao, X.; Shi, Y.; Song, R.; Giorgi, F.; Wang, Y., and Zhang, D., 2008. Reduction of future monsoon precipitation over China: comparison between a high resolution RCM simulation and the driving GCM. *Meteorology and Atmospheric Physics*,

100(1-4), 73-86.

Geyer, W. R. and Nepf, H., 1996. Tidal pumping of salt in a moderately stratified estuary. *In*: Aubrey D. G. and Friedrichs C. T. (eds.), *Buoyancy Effects on Coastal and Estuarine Dynamics*. Wiley, pp. 213-226.

Halpern, B. S.; Walbridge, S.; Selkoe, K. A.; Kappel, C. V.; Micheli, F.; D'Agrosa, C.; Bruno, J. F.; Casey, K. S.; Ebert, C., and Fox, H. E., 2008. A global map of human impact on marine ecosystems. *Science*, 319 (5865), 948-952.

Hansen, D. V. and Rattray, J. M., 1966. New dimensions in estuary classification. *Limnology and Oceanography*, 11, 319-325.

Haralambidou, K.; Sylaios, G., and Tsihrintzis, V. A., 2010. Salt-wedge propagation in a Mediterranean micro-tidal river mouth. *Estuarine, Coastal and Shelf Science*, 90(4), 174-184.

Hunkins, K., 1981. Salt dispersion in the Hudson estuary. *Journal of Physical Oceanography*, 11(5), 729-738.

Ji, D.; Yang, J.; Gao, Z., and Jia, Y., 2007. Eutrophication assessment of the western sea area in the Laizhou bay during the low water period. *Marine Environmental Science (China)*, 26(1), 78-81(Chinese with English abstract).

Jin, X. S.; Shan, X. J.; Li, X. S.; Wang, J.; Cui, Y., and Zuo, T., 2012. Long-term changes in the fishery ecosystem structure of Laizhou bay, China. *Science China Earth Sciences*, 1-9.

Kasai, A.; Kurikawa, Y.; Ueno, M.; Robert, D., and Yamashita, Y., 2010. Salt-wedge intrusion of seawater and its implication for phytoplankton dynamics in the Yura estuary, Japan. *Estuarine, Coastal and Shelf Science*, 86(3), 408-414.

Kjerfve, B., 1986. Circulation and salt flux in a well mixed estuary. *Physical of Shallow Estuaries and Bays*, (16), 22-29.

Luo, X.; Zhang, S.; Yang, J.; Pan, J.; Tian, L., and Zhang, L., 2013. Macrobenthic community in the Xiaoqing river estuary in Laizhou bay, China. *Journal of Ocean University of China*, 12(3), 366-372.

Ma, S.; Xin, F.; Cui, Y., and Qiao, X., 2004. Assessment of main pollution matter volume into the sea from yellow river and Xiaoqing river. *Marine Fisheries Research (China)*, 25(5), 47-51 (Chinese with English abstract).

Miranda, L. B. D., and Kjerfve, B., 1998. Circulation and mixing due to tidal forcing in the Bertioga channel, Sao Paulo, Brazil. *Estuaries*, 21(2), 204-214.

Miranda, L. B. D.; Olle, E. D.; Bérgamo, A. L.; Silva, L. D. S., and Andutta, F. P., 2012. Circulation and salt intrusion in the Piaçaguera channel, Santos (SP). *Brazilian Journal of Oceanography*, 1(60), 11-23.

Nepf, H. M. and Geyer, W. R., 1996. Intratidal variations in stratification and mixing in the Hudsonestuary. *Journal of Geophysical Research*, 101(C5), 12079-12086.

Officer, C. B. and Kester, D. R., 1991. On estimating the non-advective tidal exchanges and advective gravitational circulation exchanges in an estuary. *Estuarine, Coastal and Shelf Science*, 32(1), 99-103.

Pan, X.; Tang, J.; Chen, Y.; Li, J., and Zhang, G., 2011. Polychlorinated naphthalenes (PCNs) in riverine and marine sediments of the Laizhou bay area, north China. *Environmental Pollution*, 159(12), 3515-3521.

Pan, X.; Tang, J.; Li, J.; Zhong, G.; Chen, Y., and Zhang, G., 2011. Polybrominated diphenyl ethers (PBDEs) in the riverine and marine sediments of the Laizhou bay area, north China. *Journal of Environmental Monitoring*, 13(4), 886.

Park, J. K. and James, A., 1990. Mass flux estimation and mass transport mechanism in estuaries. *Limnology and Oceanography*, 35(6), 1301-1313.

Parker, B. B., 2007. Sequential tidal analysis and prediction. Center for Operational Oceanographic Products and Services. Maryland, 138.

Restrepo, J. D. and Kjerfve, B., 2002. The San Juan delta, Colombia: tides, circulations, and salt dispersion. *Continental Shelf Research*, 22(8), 1249-1267.

Richardson, L. F., 1920. The supplying of energy from and to atmospheric eddies. *Proceedings of the Royal Society of London. Series A, Containing Papers of a Mathematical and Physical Character*, 97(686), 354-373.

Siegle, E.; Schettini, C. A. F.; Klein, A. H. F., and Toldo, E. E. Jr., 2009. Hydrodynamics and suspended sediment transport in the Camboriú estuary - Brazil: pre jetty conditions. *Brazilian Journal of Oceanography*, 57(2), 123-135.

Sierra, J. P.; Sánchez-Arcilla, A.; González Del Rìo J.; Flos, J.; Movellán, E.; Mösso, C.; Martınez, R.; Rodilla, M.; Falco, S., and Romero, I., 2002. Spatial distribution of nutrients in the Ebro estuary and plume. *Continental Shelf Research*, 22(2), 361-378.

Simpson, J. H.; Gong, W. K., and Ong, J. E., 1997. The determination of the net fluxes from a mangrove estuary system. *Estuaries*, 20(1), 103-109.

Simpson, J. H.; Vennell, R., and Souza, A. J., 2001. The salt fluxes in a tidally-energetic estuary. *Estuarine, Coastal and Shelf Science*, 52(1), 131-142.

Stommel, H. and Farmer, H. G., 1952. Abrupt change in width in two-layer open channel flow. *Journal of Marine Research*, 11(2), 205-214.

Sylaios, G. K.; Tsihrintzis, V. A.; Akratos, C., and Haralambidou, K., 2006. Quantification of water, salt and nutrient exchange processes at the mouth of a Mediterranean coastal lagoon. *Environmental Monitoring and Assessment*, 119(1-3), 275-301.

Tsur, Y., 2004. *Pricing irrigation water: principles and cases from developing countries*. Washington DC: Routledge Press, 336p.

Uncles, R. J. and Jordan, M. B., 1979. Residual fluxes of water and salt at two stations in the Severn estuary. *Estuarine and Coastal Marine Science*, 9(3), 287-302.

Uncles, R. J. and Lewis, R. E., 2001. The transport of fresh water from river to coastal zone through a temperate estuary. *Journal of Sea Research*, 46(2), 161-175.

Uncles, R. J.; Elliott, R., and Weston, S. A., 1985. Observed fluxes of water, salt and suspended sediment in a partly mixed estuary. *Estuarine, Coastal and Shelf Science*, 20(2), 147-167.

Valle-Levinson, A., 2010. *Contemporary issues in estuarine physics*. New York: Cambriges University Press, 315p.

Vaz, N.; Lencart, E. S. J., and Dias, J. M., 2012. Salt fluxes in a complex river mouth system of Portugal. *PLOS One*, 7(10), e47349eng.

Wolanski, E., 2007. *Estuarine ecohydrology*. Amsterdam: Elsevier Science. 154p.

Xia, B. and Zhang, L., 2011. Carbon distribution and fluxes of 16 rivers discharging into the Bohai sea in summer. *Acta Oceanologica Sinica*, 30(3), 43–54.

Zhang, R.; Zhang, G.; Zheng, Q.; Tang, J.; Chen, Y.; Xu, W.; Zou, Y., and Chen, X., 2012. Occurrence and risks of antibiotics in the Laizhou bay, China: impacts of river discharge. *Ecotoxicology and Environmental Safety*, 80(0), 208–215.

Zhong, G.; Tang, J.; Zhao, Z.; Pan, X.; Chen, Y.; Li, J., and Zhang, G., 2011. Organochlorine pesticides in sediments of Laizhou bay and its adjacent rivers, north China. *Marine Pollution Bulletin*, 62(11), 2543–2547.

Zhuang, W. and Gao, X., 2014. Assessment of heavy metal impact on sediment quality of the Xiaoqinghe estuary in the coastal Laizhou bay, Bohai sea: inconsistency between two commonly used criteria. *Marine Pollution Bulletin*, 83(1), 352–357.